

Modeling brainstem respiratory center

From single pacemaker to network

NEUR 615 final project

Huanan Shi
Baylor College of Medicine

Abstract

Brainstem plays crucial roles in central nervous system. Breathing control center in brainstem controls and regulates autonomous respiratory functions, from basic rhythm generation to other more advanced fine adjustment. However, how respiratory center working is still elusive. Studies from last several decades showed distinct subpopulations of neurons in different regions may play specific roles.

A cluster of several thousand neurons in ventral-lateral medulla, termed as pre-Bötzinger complex (preBötC), are considered to generate autonomic respiratory rhythms. The preBötC initiates breathing by recurrently activating premotor and motor neurons of the respiratory muscles. They also crosstalk with chemosensitive neurons and other cortex regions.

With recent finding in respiratory center, previous preBötC model requires modification. Thus, in this project, I first modeled a simple pacemaker in preBötC using Hodgkin-Huxley model activation function. Then, a network model of preBötC is generated to mimic the network for rhythm generation. At the end, preBötC pacemaker network was linked with chemosensitive parafacial regions to optimize the rhythm generator by the chemosensitivity.

The network model can be used to mimic experiment data under hypoxia and hypercapnia situation and will be able to predict physiological parameters of respiratory function.

I. Introduction and background

Contractions of the diaphragm and external intercostal muscles expand the chest cavity and rib cage to draw the air into the lungs, and give rise to breath. The respiratory system helps maintain the blood $p\text{CO}_2/p\text{H}$ and $p\text{O}_2$ levels within a narrow physiological range, while a wide range of behaviors, such as vocalization, exercise, coughing, swallowing and *et cetera*, are conducted. Disturbances to the respiratory function have significant consequences and may lead to death.

To maintain homeostasis, hypercapnic and hypoxia chemoreflexes are acute, which immediately increase ventilation in response to increased CO_2 and decreased O_2 levels, respectively. Abnormalities of both chemoreflexes are considered to be underlying factors in fatalities in a wide range of disorders with respiratory dysfunctions, including Sudden Infant Death Syndrome, Rett Syndrome, Sudden Unexpected Death Syndrome, sleep apnea, and more. The stability of breathing and intrinsic respiratory rhythm is regulated in a complex network of nuclei in the brainstem.

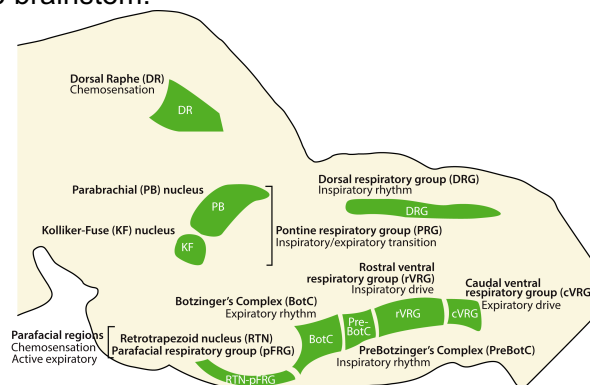


Figure 1 Brainstem Respiratory Center

Decades of studies have identified a number of key nucleus in brainstem (Figure 1). The ventral respiratory column (VRC) consists of the retrotrapezoid nucleus (RTN) /parafacial respiratory group(pFRG), the Böttinger Complex (BötC), the Pre-Böttinger Complex (preBötC), the post-inspiratory complex, the rostral ventral respiratory group (rVRG) and the caudal ventral respiratory group (cVRG). Outside of VRC, the Kölliker-Fuse nucleus, parabrachial complex form pontine respiratory group in dorsal pons.

The RTN/pFRG are located at parafacial region (pF), which are important for central CO_2 -chemoreception and for gating active expiration. Disinhibition of lateral parafacial nuclei (pF_L) led to active expiration, while ventral parafacial nuclei (pF_V) provides tonic drive coordinated with hypercapnia, hypoxia or stimulation of pF_V (Figure 2)¹. The preBötC functions as respiratory pacemaker for inspiratory rhythm generation. It activates the tongue protrussor muscles via hypoglossal nerves (pXII) and then maintains throughout inspiration to prevent obstruction of the oropharyngeal airway². It mostly contains spontaneous pacemakers but also crosstalk with more advanced cortex regions³. Recent study also showed that preBötC pacemakers send inhibitory signal to pF_L and thereby alters the electrophysiological properties of pXII and also gives an inhibitory feedback to preBötC via BötC interneurons (Figure 2)¹.

In this project, we ignored the pF_V tonic drive and only modeled the interaction between preBötC and pF_L.

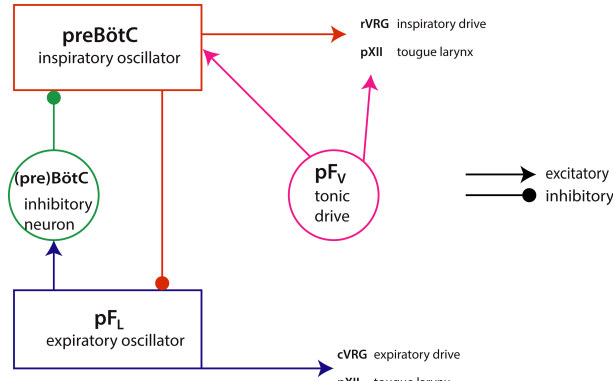


Figure 2 Rhythm Generation Network (modified from Huckstepp et al, JNeuro 2015)

II. Methods

1. Single pacemaker model

Butera *et al* proposed an inspiratory pacemaker model with fast-activating, slow inactivation Na^+ current^{4,5}. It recruited a simple Hodgkin-Huxley model with fast changing membrane potential V_m and gating variable n for I_K .

State variables evolve according to nonlinear ordinary differential equation:

$$C \dot{V}_m = -I_{\text{NaP}} - I_{\text{Na}} - I_K - I_{L(K)} - I_{L(\text{Na})} - I_{\text{Leak}} \dots (1)$$

$$\dot{n} = \frac{n_\infty(V_m) - n}{\tau_n(V_m)} \dots (2)$$

$$\dot{h} = \frac{h_\infty(V_m) - h}{\tau_h(V_m)} \dots (3)$$

For gating variables n, h :

$$x_\infty(V_m) = \frac{1}{1 + e^{\frac{V_m - \theta_x}{\sigma_x}}}, x = n, h \dots (4)$$

$$\tau_x(V_m) = \frac{\bar{\tau}_x}{\cosh(\frac{V_m - \theta_x}{2\sigma_x})}, x = n, h \dots (5)$$

Action potential I_{Na} and I_K currents are described by:

$$I_{\text{Na}} = \bar{g}_{\text{Na}} m_\infty^3(V_m) (1 - n) (V_m - E_{\text{Na}}) \dots (6)$$

$$I_K = \bar{g}_K n^4(V_m) (V_m - E_K) \dots (7)$$

where \bar{g}_{Na} and \bar{g}_K are maximal conductance, $m_\infty(V_m)$ is voltage-dependent activation and E_{Na} and E_K are Nernst potential.

I_{NaP} is described by:

$$I_{\text{NaP}} = \bar{g}_{\text{NaP}} p_\infty(V_m) h (V_m - E_{\text{Na}}) \dots (8)$$

with \bar{g}_{NaP} as maximal conductance and $p_\infty(V_m)$ as instantaneous activation. The leakage currents are divided into K^+ and Na^+ component with $I_{L(K)}$ and $I_{L(\text{Na})}$ respectively, defined as:

$$I_{L(K)} = g_{L(K)}(V_m - E_K) \quad \dots (9)$$

$$I_{L(Na)} = g_{L(Na)}(V_m - E_{Na}) \quad \dots (10)$$

with non-gated conductance $g_{L(K)}$ and $g_{L(Na)}$ respectively.

Non-NDMA excitatory amino-acid receptor tonic input $I_{tonic(e)}$ is described as:

$$I_{tonic(e)} = g_{tonic(e)}(V_m - E_{syn(e)}) \quad \dots (11)$$

with synaptic conductance $g_{tonic(e)}$ and Nernst potential $E_{syn(e)}$. In single cell model, $g_{tonic(e)} = 0$.

Standard parameters for single cell model are $C = 21 \text{ pF}$, $\bar{g}_{Na} = 28 \text{ nS}$, $\bar{g}_K = 11.2 \text{ nS}$, $\bar{g}_{NaP} = 2.4 \text{ nS}$, $g_{L(K)} = 2.4 \text{ nS}$, $g_{L(Na)} = 0.4 \text{ nS}$, $E_{Na} = 50 \text{ mV}$, $E_K = -85 \text{ mV}$, $E_{syn(e)} = 0 \text{ mV}$, $\theta_m = -34 \text{ mV}$, $\sigma_m = -5 \text{ mV}$, $\theta_n = -29 \text{ mV}$, $\sigma_n = -4 \text{ mV}$, $\theta_p = -40 \text{ mV}$, $\sigma_p = -6 \text{ mV}$, $\theta_h = -48 \text{ mV}$, $\sigma_h = 6 \text{ mV}$, $\tau_n = 10 \text{ ms}$, $\tau_h = 10^4 \text{ ms}$, and $g_{tonic(e)} = 0 \text{ nS}$.

2. Pacemaker network

For N heterogeneous pacemaker network, coupled by non-NMDA fast excitatory synapse, phasic synaptic input $I_{syn(e)}$ was added into Eq.1. Neuron j receives the excitatory inputs from $N - 1$ non- j cells⁴⁻⁶:

$$I_{syn(e)} = \left(\sum_{i=1}^{N-1} \bar{g}_{syn(e),i,j} s_i \right) (V_m - E_{syn(e)}) \quad \dots (12)$$

$$\dot{s}_i = \frac{(1 - s_i) s_{\infty}(V_{mi}) - k_r s_i}{\tau_s} \quad \dots (13)$$

where $\bar{g}_{syn(e),i,j}$ represent synaptic conductance between neuron i and j . The presynaptic action potential activates s_i , the synaptic gating variable, with $\tau_s = 5 \text{ ms}$ and $k_r = 1$ in respiratory neurons. For synaptic gating variable, $\theta_s = -10 \text{ mV}$, $\sigma_s = -5 \text{ mV}$.

To fulfill the heterogeneity of pacemaker neurons, the parameters \bar{g}_{NaP} , $g_{L(K)}$ and $g_{syn(e)}$ were randomly determined from normal distributions.

3. Follower cells

In our network described in Figure 2, there are two types of follower cells, pacemaker and non-pacemaker neurons. The hypoglossal nerve can be treated as non-pacemaker neuron, in which $\bar{g}_{NaP} = 0$. The lateral parafacial neurons contribute to active excitatory rhythm generation, and thereby serve as one type of pacemaker. Since inspiratory pacemaker neurons inhibit lateral parafacial neurons, a phasic synaptic current from preBötC with opposite direction was incorporated into Eq.1. The probability of synaptic connection between preBötC pacemaker neurons and follower cells was 0.5.

The lateral parafacial neurons in turn inhibit preBötC via a non-pacemaker interneuron. The lateral parafacial neurons also contribute to pXII action potential.

III. Results

Figure 3 showed the results of single cell model given $E_K = -75 \text{ mV}$ and resting membrane potential $V_m = -56 \text{ mV}$. Figure 4 gave one example neuron of coupled pacemaker network, where $g_{\text{tonic}(e)} = 0.035 \text{ nS}$, $g_{\text{syn}(e)} \sim N(0.1, 0.025)$, and resting membrane potential $V_m = -56 \text{ mV}$.

Then we modeled respiratory network shown in Figure 2, in which we ignored ventral parafacial tonic drive and BötC interneuron. Results were shown in Figure 5. The results are similar to the experimental data. And we also compared the burst properties among PreBötC inspiratory pacemaker, pFL active expiratory pacemaker, and hypoglossal nerve neurons (Figure 6), which are as expected.

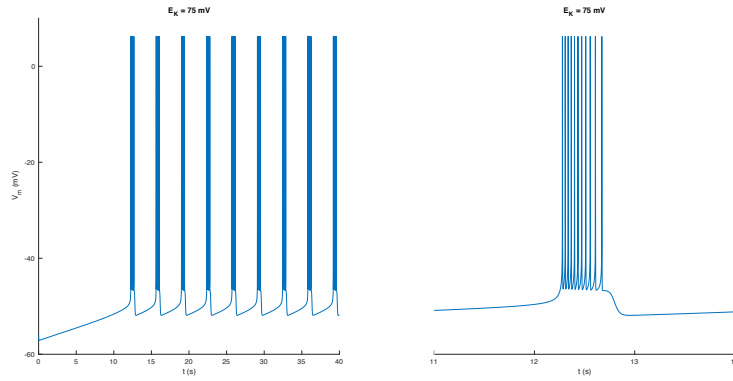


Figure 3 Single Pacemaker model with resting membrane potential 56 mV

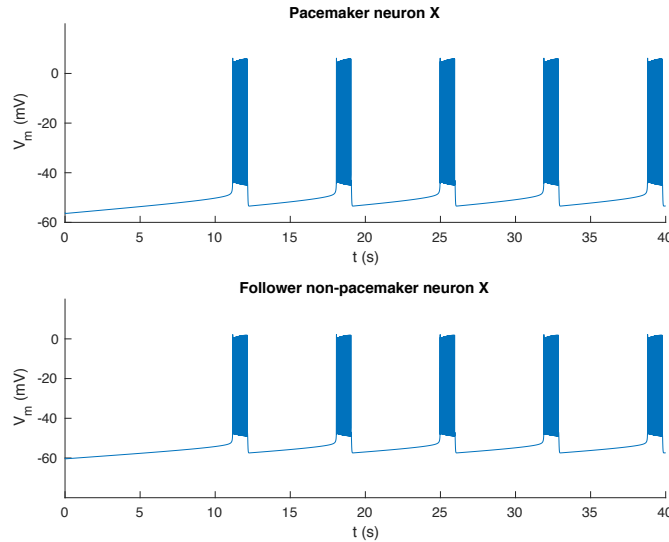


Figure 4 Pacemaker Neuron X with $g_{\text{tonic}(e)} = 0.035 \text{ nS}$, $g_{\text{syn}(e)} \sim N(0.1, 0.025)$

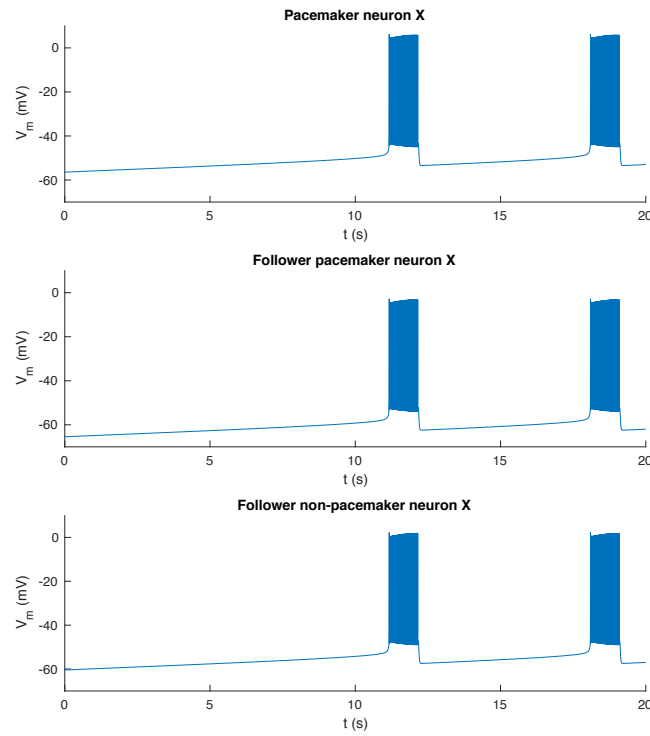


Figure 5 Respiratory network with pacemaker interneuron

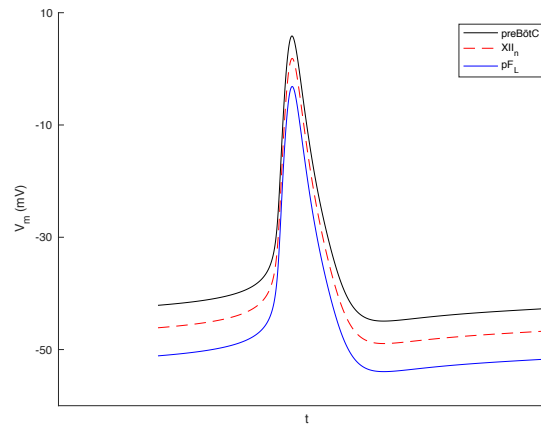


Figure 6 Burst Comparison of PreBötC inspiratory pacemaker, pF_L active expiratory pacemaker and $pXII$ nerve neurons

IV. Limitation

The models discussed above are simplified. In reality, all the parameters may be different among neuron, and all pacemakers may not be coupled well. Also, other factors and other interneurons were ignored. They may play important roles in respiratory control.

V. References:

- 1 Huckstepp, R. T., Cardoza, K. P., Henderson, L. E. & Feldman, J. L. Role of parafacial nuclei in control of breathing in adult rats. *J Neurosci* **35**, 1052-1067, doi:10.1523/JNEUROSCI.2953-14.2015 (2015).
- 2 Smith, J. C., Abdala, A. P., Borgmann, A., Rybak, I. A. & Paton, J. F. Brainstem respiratory networks: building blocks and microcircuits. *Trends Neurosci* **36**, 152-162, doi:10.1016/j.tins.2012.11.004 (2013).
- 3 Yackle, K. *et al.* Breathing control center neurons that promote arousal in mice. *Science* **355**, 1411-1415, doi:10.1126/science.aai7984 (2017).
- 4 Butera, R. J., Jr., Rinzel, J. & Smith, J. C. Models of respiratory rhythm generation in the pre-Botzinger complex. I. Bursting pacemaker neurons. *J Neurophysiol* **82**, 382-397 (1999).
- 5 Del Negro, C. A., Johnson, S. M., Butera, R. J. & Smith, J. C. Models of respiratory rhythm generation in the pre-Botzinger complex. III. Experimental tests of model predictions. *J Neurophysiol* **86**, 59-74 (2001).
- 6 Butera, R. J., Jr., Rinzel, J. & Smith, J. C. Models of respiratory rhythm generation in the pre-Botzinger complex. II. Populations Of coupled pacemaker neurons. *J Neurophysiol* **82**, 398-415 (1999).

VI. Appendix

```
%parameters
C = 21;
g_Na_max = 28;
g_K_max = 11.2;
g_NaP_max = 2.4;
gL_K = 2.4;
gL_Na = 0.4;
E_Na = 50;
E_K = -75;
theta_m = -34;
theta_n = -29;
theta_h = -48;
theta_p = -40;
s_m = -5;
s_n = -4;
s_h = 6;
s_p = -6;
tau_n_max = 10;
tau_h_max = 10^4;
%single neuron
T = 4*10^4;
dt = 0.01;
N = T/dt;
n = zeros(1,N);
h = n;
V_m = n;
V_m(1) = -56;
n_max = 1/(1+exp((V_m(1)-theta_n)/s_n));
tau_n = tau_n_max/(cosh((V_m(1)-theta_n)/2/s_n));
h_max = 1/(1+exp((V_m(1)-theta_h)/s_h));
tau_h = tau_h_max/(cosh((V_m(1)-theta_h)/2/s_h));

for j = 2:N
    dn = dt*(n_max-n(j-1))/tau_n;
    dh = dt*(h_max-h(j-1))/tau_h;
    n(j) = dn+n(j-1);
    h(j) = dh+h(j-1);
    m_max = 1/(1+exp((V_m(j-1)-theta_m)/s_m));
    I_Na = g_Na_max*m_max^3*(1-n(j))*(V_m(j-1)-E_Na);
    I_K = g_K_max*n(j)^4*(V_m(j-1)-E_K);
    p_max = 1/(1+exp((V_m(j-1)-theta_p)/s_p));
```



```

I_NaP = g_NaP_max*p_max*h(j)*(V_m(j-1)-E_Na);
IL_K = gL_K*(V_m(j-1)-E_K);
IL_Na = gL_Na*(V_m(j-1)-E_Na);
dV = -dt*(I_NaP+I_Na+I_K+IL_K+IL_Na)/C;
V_m(j)=V_m(j-1)+dV;
n_max = 1/(1+exp((V_m(j)-theta_n)/s_n));
tau_n = tau_n_max/(cosh((V_m(j)-theta_n)/2/s_n));
h_max = 1/(1+exp((V_m(j)-theta_h)/s_h));
tau_h = tau_h_max/(cosh((V_m(j)-theta_h)/2/s_h));
end
t = linspace(0,T/1000,N);
subplot(1,2,1)
plot(t,V_m);
title('E_K = 75 mV')
xticks(0:5:40)
yticks(-60:20:0)
xlabel('t (s)')
ylabel('V_m (mV)')
box off
subplot(1,2,2)
t1 = 10*10^3/dt;
t2 = 15*10^3/dt;
plot(t(t1:t2),V_m(t1:t2));
title('E_K = 75 mV')
xticks(10:1:15)
xlabel('t (s)')
xlim([11 14])
yticks([])
box off
%Pacemaker network
figure(2)
N_c = 50;
s = zeros(1,N_c);
g_syn = normrnd(0.1,0.025,1,N_c);
g_tonic = 0.035;
theta_s = -10;
tau_s = 5;
kr = 1;
s_s = -5;
E_syn = 0;
n = zeros(1,N);
h = n;
V_m = n;
V_m(1) = -56;
V_m_f = V_m;
V_m_f(1) = -60;
n_max = 1/(1+exp((V_m(1)-theta_n)/s_n));
tau_n = tau_n_max/(cosh((V_m(1)-theta_n)/2/s_n));
h_max = 1/(1+exp((V_m(1)-theta_h)/s_h));
tau_h = tau_h_max/(cosh((V_m(1)-theta_h)/2/s_h));

for j = 2:N
    dn = dt*(n_max-n(j-1))/tau_n;
    dh = dt*(h_max-h(j-1))/tau_h;
    n(j) = dn+n(j-1);
    h(j) = dh+h(j-1);
    m_max = 1/(1+exp((V_m(j-1)-theta_m)/s_m));
    I_Na = g_Na_max*m_max^3*(1-n(j))*(V_m(j-1)-E_Na);
    I_K = g_K_max*n(j)^4*(V_m(j-1)-E_K);
    p_max = 1/(1+exp((V_m(j-1)-theta_p)/s_p));
    I_NaP = g_NaP_max*p_max*h(j)*(V_m(j-1)-E_Na);
    IL_K = gL_K*(V_m(j-1)-E_K);
    IL_Na = gL_Na*(V_m(j-1)-E_Na);
    s_max = 1/(1+exp((V_m(j-1)-theta_s)/s_s));
    for i = 1:N_c
        ds = dt*((1-s(i))*s_max-kr*s(i))/tau_s;
        s(i)=ds+s(i);
    end
    I_syn_f = binornd(1,0.5)*g_f*s(N_c)*(V_m_f(j-1)-E_syn);
    dV_f = -dt*(I_Na+I_K+IL_K+IL_Na+I_syn_f)/C;
    V_m_f(j)=V_m_f(j-1)+dV;
    I_syn = sum(g_syn(1:N_c-1).*s(1:N_c-1))*(V_m(j-1)-E_syn);
    I_tonic = g_tonic*(V_m(j-1)-E_syn);
    dV = -dt*(I_NaP+I_Na+I_K+IL_K+IL_Na+I_syn+I_tonic)/C;
    V_m(j)=V_m(j-1)+dV;
    n_max = 1/(1+exp((V_m(j)-theta_n)/s_n));
    tau_n = tau_n_max/(cosh((V_m(j)-theta_n)/2/s_n));
    h_max = 1/(1+exp((V_m(j)-theta_h)/s_h));

```

```

        tau_h = tau_h_max/(cosh((V_m(j)-theta_h)/2/s_h));
    end
    t = linspace(0,T/1000,N);
    subplot(2,1,1)
    plot(t,V_m);
    title('Pacemaker neuron X')
    xticks(0:5:40)
    yticks(-60:20:0)
    xlabel('t (s)')
    ylabel('V_m (mV)')
    box off
    subplot(2,1,2)
    plot(t,V_m_f)
    xticks(0:5:40)
    yticks(-60:20:0)
    xlabel('t (s)')
    ylabel('V_m (mV)')
    title('Follower non-pacemaker neuron X')
    box off
    %with inhibitory input
    figure(3)
    T = 2*10^4;
    N = T/dt;
    n = zeros(1,N);
    h = n;
    V_m = n;
    V_m(1) = -56;
    V_m_l = n;
    V_m_l(1) = -65;
    V_m_f = n;
    V_m_f(1) = -60;
    n_max = 1/(1+exp((V_m(1)-theta_n)/s_n));
    tau_n = tau_n_max/(cosh((V_m(1)-theta_n)/2/s_n));
    h_max = 1/(1+exp((V_m(1)-theta_h)/s_h));
    tau_h = tau_h_max/(cosh((V_m(1)-theta_h)/2/s_h));
    s_l = 0;
    for j = 2:N
        dn = dt*(n_max-n(j-1))/tau_n;
        dh = dt*(h_max-h(j-1))/tau_h;
        n(j) = dn+n(j-1);
        h(j) = dh+h(j-1);
        m_max = 1/(1+exp((V_m(j-1)-theta_m)/s_m));
        I_Na = g_Na_max*m_max^3*(1-n(j))*(V_m(j-1)-E_Na);
        I_K = g_K_max*n(j)^4*(V_m(j-1)-E_K);
        p_max = 1/(1+exp((V_m(j-1)-theta_p)/s_p));
        I_NaP = g_NaP_max*p_max*h(j)*(V_m(j-1)-E_Na);
        IL_K = gL_K*(V_m(j-1)-E_K);
        IL_Na = gL_Na*(V_m(j-1)-E_Na);
        s_max = 1/(1+exp((V_m(j-1)-theta_s)/s_s));
        for i = 1:N_c
            ds = dt*((1-s(i))*s_max-kr*s(i))/tau_s;
            s(i)=ds+s(i);
        end
        g_l=binornd(1,0.5)*normrnd(0.1,0.025);
        I_syn_l = g_l*s(N_c)*(V_m_l(j-1)-E_syn);
        I_tonic_l = g_tonic*(V_m(j-1)-E_syn);
        dV_l = -dt*(I_NaP+I_Na+I_K+IL_K+IL_Na-I_syn_l+I_tonic_l)/C;
        V_m_l(j)=V_m_l(j-1)+dV;
        s_l_max = 1/(1+exp((V_m_l(j-1)-theta_s)/s_s));
        ds_l = dt*((1-s_l)*s_l_max-kr*s_l)/tau_s;
        s_l = ds_l+s_l;
        g_f=normrnd(1,0.25,1,2).*binornd(1,0.5,1,2);
        I_syn_f = sum(g_f.*[s(N_c) s_l])*(V_m_f(j-1)-E_syn);
        dV_f = -dt*(I_Na+I_K+IL_K+IL_Na+I_syn_f)/C;
        V_m_f(j)=V_m_f(j-1)+dV;
        I_syn = (sum(g_syn(1:N_c-1).*s(1:N_c-1))-g_l*s_l)*(V_m(j-1)-E_syn);
        I_tonic = g_tonic*(V_m(j-1)-E_syn);
        dV = -dt*(I_NaP+I_Na+I_K+IL_K+IL_Na+I_syn+I_tonic)/C;
        V_m(j)=V_m(j-1)+dV;
        n_max = 1/(1+exp((V_m(j)-theta_n)/s_n));
        tau_n = tau_n_max/(cosh((V_m(j)-theta_n)/2/s_n));
        h_max = 1/(1+exp((V_m(j)-theta_h)/s_h));
        tau_h = tau_h_max/(cosh((V_m(j)-theta_h)/2/s_h));
    end
    t = linspace(0,T/1000,N);
    subplot(3,1,1)
    plot(t,V_m);
    title('Pacemaker neuron X')

```

```

xticks(0:5:20)
yticks(-60:20:0)
xlabel('t (s)')
ylabel('V_m (mV)')
ylim([-70 10])
box off
subplot(3,1,2)
plot(t,V_m_l);
title('Follower pacemaker neuron X')
xticks(0:5:20)
yticks(-60:20:0)
xlabel('t (s)')
ylabel('V_m (mV)')
ylim([-70 10])
box off
subplot(3,1,3)
plot(t,V_m_f)
xticks(0:5:20)
yticks(-60:20:0)
xlabel('t (s)')
ylabel('V_m (mV)')
title('Follower non-pacemaker neuron X')
ylim([-70 10])
box off
figure(4)
t3 = 12*10^3/dt;
t4 = 12.02*10^3/dt;
plot(t(t3:t4),V_m(t3:t4),'k-',t(t3:t4),V_m_f(t3:t4),'r--',t(t3:t4),V_m_l(t3:t4),'b-')
xticks([])
xlabel('t')
yticks(-50:20:10)
ylabel('V_m (mV)')
legend('preBötC', 'XII_n', 'pF_L')
box off

```